Template-Directed Preparation of Macroporous Polymers with Oriented and Crystalline Arrays of Voids

P. Jiang,[†,§] K. S. Hwang,[†,§] D. M. Mittleman,[‡,§] J. F. Bertone,[†,§] and V. L. Colvin*[,†,§]

Contribution from the Department of Chemistry, Department of Electrical and Computer Engineering, and Rice Quantum Institute, Rice University, Houston, Texas 77005

Received February 4, 1999. Revised Manuscript Received October 12, 1999

Abstract: The fabrication of polymeric materials with ordered submicron-sized void structures is potentially valuable for many separation technologies as well as for emerging optical applications. This paper reports the preparation of macroporous polymer membranes with regular voids and the characterization of their diffractive optical properties. These materials are made using a colloidal crystal template of silica microspheres; the air between the spheres can be replaced by monomers that can be subsequently polymerized. The use of silica microspheres as templates makes it possible to employ chemical rather than thermal methods for template removal. For this reason, polymers as diverse as polyurethane and polystyrene can be used to create free-standing macroporous films, with thickness ranging from 0.5 to 50 μm. Scanning electron microscopy of these samples indicates a well-formed porous structure consisting of voids ranging in diameter from 200 to 400 nm. These large cavities are not isolated, but rather interconnected by a network of monodisperse smaller pores ($d = 50-130$ nm) whose size can be controlled by varying the polymerization temperature. These membranes exhibit striking optical properties due to the periodic arrangement of air spheres in the polymer medium. Normal-incidence transmission measurements of these samples are compared to a theoretical model based on a scalar wave approximation. This model assumes an ordered structure of close-packed, three-dimensional air spheres. The good agreement between theory and experiment provides additional evidence of the long-range order of these samples.

Introduction

Macroporous materials, those with pore diameters greater than 50 nm,[1] have a wide range of applications in chemistry. Macroporous polymers, in particular, can be used as catalytic surfaces and supports,[2,3] separation and adsorbent media,[4−6] biomaterials,[7−10] chromatographic materials,[11−13] and thermal, acoustic, and electrical insulators.[14−17] In nearly every case, the utility of the porous system is a sensitive function of the internal pore diameters, their distribution,[18−21] and their morphology.[11] As a result, most of the synthetic approaches to creating these materials, both polymeric and inorganic, have focused on creating internal voids with monodisperse and controllable diameters.[1,22,23] Toward this end, this paper describes a templating strategy for fabricating such materials, with voids ranging from 50 to 500 nm in diameter.

The motivation in this work is the growth of samples suitable for optical characterization. The materials described below are arrays of spherical air voids embedded in a host polymer matrix, exhibiting crystalline order over length scales as long as 1 cm. Since the voids have diameters of ~0.5 μm, the structure acts as a diffractive optic for visible light. Recently, these diffractive properties have received considerable attention, since theoretical modeling of photonic behavior has illustrated that control over the symmetry and the host matrix allow very strong and specific optical properties to be engineered.[24−28] Numerous optical applications have been proposed for materials exhibiting long-range three-dimensional dielectric periodicity, including for the

[†] Department of Chemistry.
[‡] Department of Electrical and Computer Engineering.
[§] Rice Quantum Institute.

(1) Wijnhoven, J. E. G. J.; Vos, W. L. *Science* **1998**, *281*, 802.
(2) Tanev, P. T.; Chibwe, M.; Pinnavaia, T. J. *Nature* **1994**, *368*, 321.
(3) Deleuze, H.; Schultze, X.; Sherrington, D. C. *Polymer* **1998**, *39*, 6109.
(4) Bhave, R. R. *Inorganic Membranes: Synthesis, Characteristics and Applications*; Van Nostrand Reinhold: New York, 1991.
(5) Lewandowski, K.; Murer, P.; Svec, F.; Frechet, J. M. J. *Anal. Chem.* **1998**, *70*, 1629.
(6) Akolekar, D. B.; Hind, A. R.; Bhargava, S. K. *J. Colloid Interface Sci.* **1998**, *199*, 92.
(7) Maquet, V.; Jerome, R. *Mater. Sci. Forum* **1997**, *250*, 15.
(8) Peters, M. C.; Mooney, D. J. *Mater. Sci. Forum* **1997**, *250*, 43.
(9) Bancel, S.; Hu, W. S. *Biotechnol. Prog.* **1996**, *12*, 398.
(10) Schugens, C.; Maquet, V.; Grandfils, C.; Jerome, R.; Teyssie, P. *Polymer* **1996**, *37*, 1027.
(11) Tennikov, M. B.; Gazdina, N. V.; Tennikova, T. B.; Svec, F. *J. Chromatogr. A* **1998**, *798*, 55.
(12) Palm, A.; Novotny, M. V. *Anal. Chem.* **1997**, *69*, 4499.
(13) Xie, S.; Svec, F.; Frechet, J. M. J. *J. Chromatogr. A* **1997**, *775*, 65.
(14) Litovsky, E.; Shapiro, M.; Shavit, A. *J. Am. Ceram. Soc.* **1996**, *79*, 1366.
(15) Seino, H.; Haba, O.; Mochizuki, A.; Yoshioka, M.; Ueda, M. *High Perform. Polym.* **1997**, *9*, 333.
(16) Senkevich, J. J.; Desu, S. B. *Appl. Phys. Lett.* **1998**, *72*, 258.
(17) Sedev, R.; Ivanova, R.; Kolarov, T.; Exerowa, D. *J. Dispersion Sci. Technol.* **1997**, *18*, 751.
(18) Imhof, A.; Pine, D. J. *Nature* **1997**, *389*, 948.
(19) Imhof, A.; Pine, D. J. *Adv. Mater.* **1998**, *10*, 697.
(20) Perrin, P. *Langmuir* **1998**, *14*, 5977.
(21) Widawski, G.; Rawiso, M.; Francois, B. *Nature* **1994**, *369*, 387.
(22) Park, S. H.; Xia, Y. *Chem. Mater.* **1998**, *10*, 1745.
(23) Velev, O. D.; Jede, T. A.; Lobo, R. F.; Lenhoff, A. M. *Nature* **1997**, *389*, 447.
(24) Joannopoulos, J. D.; Villeneuve, P. R.; Fan, S. *Nature* **1997**, *387*, 830.
(25) Soukoulis, C. M. *Photonic Band Gap Materials*; Kluwen: Dordrecht, 1996.
(26) Yablonovitch, E. *J. Opt. Soc. Am. B* **1993**, *10*, 283.
(27) Joannopoulos, J. D.; Meade, R. D.; Winn, J. N. *Photonic Crystals: Molding the Flow of Light*; Princeton University Press: Princeton, 1995.
(28) Sozuer, H. S.; Haus, J. W. *J. Opt. Soc. Am. B* **1993**, *10*, 296.

10.1021/ja9903476 CCC: $18.00
Published on Web 11/30/1999

control of spontaneous emission rates,[29−32] substrates for planar waveguides,[33] infrared filters,[34] and linear and nonlinear optics and chemical sensors.[35−37] In most of these examples the materials are diffractive only in the infrared and microwave region because of the limitations of lithographic processing. In contrast, chemically prepared macroporous materials have no intrinsic limit on the size of the pores, and thus offer a route to creating photonic materials operating at visible, ultraviolet, and even soft X-ray wavelengths. However, to be useful in optical technologies, an ordered macroporous sample must meet a number of stringent material requirements. The sample must be of high optical quality (no cracks or bubbles), cast as a film of controlled thickness on an optical substrate, and uniform over a square centimeter or more.

A number of techniques have been developed for the fabrication of well-controlled macroporous polymer materials suitable for nonoptical applications. These include ion-track etched polymers,[38] chemically induced phase separation,[39,40] self-assembly of block copolymers,[21] and copolymerization methods.[41−44] While these methods do lead to the formation of high-quality macroporous polymers, they do not provide the long-range crystalline order and sample format required for optical applications. For these requirements, methods that rely on the self-assembly of a sacrificial template to define the porous structure are more suitable. Work in the past few years has demonstrated the utility of self-organizing systems as templates for the growth of a second material. These include surfactants,[45] biological systems,[46] liquid-droplet surfaces,[47] and emulsions.[18,19] Many of these systems are capable of producing macroporous materials of both polymers and inorganic oxides with pore sizes $\geq$ 50 nm.[18,19,46,48,49] However, in these instances the templates are polycrystalline, and the resulting samples lack the long-range order and uniformity necessary for optical characterization.

A more suitable template for the production of optical materials is an array of polymer or silica spheres which, even before templating, exhibits diffractive properties. This has been demonstrated recently by several examples in which thick gravity-sedimented colloidal crystals or thin colloidal monolayers served as scaffolds for the production of inorganic[1,23,50−52] and metallic[53] macroporous materials. In a few instances the samples were of high enough quality to obtain optical data which illustrated the crystallinity of the porous structure.[1,52] Extending this method to the production of polymeric systems has also been recently reported.[22,52,54−56] For example, Xia et al. used latex and silica spheres as templates for forming ultrathin ($d <$ 5 μm) three-dimensional macroporous poly(urethane) membranes.[22,54,55] Although no optical characterization was reported, this result demonstrates the potential of using colloids in template-directed syntheses, especially of macroporous polymers.

The aim of this work is to develop a versatile templating strategy for creating macroporous polymer films appropriate for quantitative comparison with standard models of diffractive optics. We chose to work with polymers, rather than inorganic matrices, because such materials may extend the use of diffractive optics into applications that require light-weight and/or low-cost materials.[57−61] In addition, the polymer-curing process involves much less volume shrinkage than the corresponding precursor decomposition used to make inorganic systems.[62] This allows for the formation of large area ($\sim$1 cm^2) samples which can be cast as films on optical substrates. Finally, although polymeric refractive indices are lower than those of many inorganic materials, an ordered lattice of air spheres in a polymer is predicted to exhibit photonic band gap behavior, albeit over a smaller range of wavelengths and incident angles than the corresponding inorganic film.[27] Even a partial band gap, such as the one predicted by theory for these materials, is a useful property in numerous linear optical applications ranging from wavelength rejection filters[34,63,64] to optics for distributed feedback lasers.[65,66]

The macroporous polymer films in this work are formed around silica colloidal crystal templates, which are themselves designed for optical applications. These templates were grown following a method that casts colloidal films with controlled thickness in planar formats;[67] use of these high quality templates

(29) Yablonovitch, E. *Phys. Rev. Lett.* **1987**, *58*, 2059.
(30) John, S. *Phys. Rev. Lett.* **1987**, *58*, 2486.
(31) Petrov, E. P.; Bogomolov, V. N.; Kalosha, I. I.; Gaponenko, S. V. *Phys. Rev. Lett.* **1998**, *81*, 77.
(32) Martorell, J.; Lawandy, N. M. *Phys. Rev. Lett.* **1991**, *66*, 887.
(33) Lin, S. Y.; Chow, E.; Hietala, V.; Villeneuve, P. R.; Joannopoulos, J. D. *Science* **1998**, *282*, 274.
(34) Gupta, S.; Tuttle, G.; Sigalas, M.; Ho, K. M. *Appl. Phys. Lett.* **1997**, *71*, 2412.
(35) Asher, S. A.; Holtz, J.; Weissman, J.; Pan, G. *MRS Bull.* **1998**, *23*, 44.
(36) Holtz, J. H.; Asher, S. A. *Nature* **1997**, *389*, 829.
(37) Martorell, J.; Vilaseca, R.; Corbalan, R. *Phys. Rev. A* **1997**, *55*, 4520.
(38) Yoshida, M.; Asano, M.; Suwa, T.; Reber, N.; Spohr, R.; Katakai, R. *Adv. Mater.* **1997**, *9*, 757.
(39) Kiefer, J.; Hilborn, J. G.; Hedrick, J. L. *Polymer* **1996**, *37*, 5715.
(40) Kiefer, J.; Hilborn, J. G.; Maanson, J. A. E.; Leterrier, Y.; Hedrick, J. L. *Macromolecules* **1996**, *29*, 4158.
(41) Lewandowski, K.; Svec, F.; Frechet, J. M. J. *J. Appl. Polym. Sci.* **1998**, *67*, 597.
(42) Svec, F.; Frechet, J. M. J. *Macromolecules* **1995**, *28*, 7580.
(43) Peters, E. C.; Svec, F.; Frechet, J. M. J. *Chem. Mater.* **1997**, *9*, 1898.
(44) Viklund, C.; Ponten, E.; Glad, B.; Irgum, K.; Hoerstedt, P.; Svec, F. *Chem. Mater.* **1997**, *9*, 463.
(45) Kresge, C. T.; Leonowicz, M. E.; Roth, W. J.; Vartuli, J. C.; Beck, J. S. *Nature* **1992**, *359*, 710.
(46) Davis, S. A.; Burkett, S. L.; Mendelson, N. H.; Mann, S. *Nature* **1997**, *385*, 420.
(47) Huck, W. T. S.; Tien, J.; Whitesides, G. M. *J. Am. Chem. Soc.* **1998**, *120*, 8267.
(48) Coombs, N.; Khushalani, D.; Oliver, S.; Ozin, G. A.; Shen, G. C.; Sokolov, I.; Yang, H. *J. Chem. Soc., Dalton Trans.* **1997**, *21*, 3941.
(49) Caruso, R. A.; Giersig, M.; Willig, F.; Antonietti, M. *Langmuir* **1998**, *14*, 6333.
(50) Velev, O. D.; Jede, T. A.; Lobo, R. F.; Lenhoff, A. M. *Chem. Mater.* **1998**, *10*, 3597.
(51) Holland, B. T.; Blanford, C.; Stein, A. *Science* **1998**, *281*, 538.
(52) Zakhidov, A. A.; Baughman, R. H.; Iqbal, Z.; Cui, C.; Khayyrullin, I.; Dantas, O.; Marti, J.; Ralchenko, V. G. *Science* **1998**, *282*, 897.
(53) Jiang, P.; Cizeron, J.; Bertone, J. F.; Colvin, V. L. *J. Am. Chem. Soc.* **1999**, *121*, 7957.
(54) Park, S. H.; Xia, Y. *Adv. Mater.* **1998**, *10*, 1045.
(55) Gates, B.; Yin, Y.; Xia, Y. *Chem. Mater.* **1999**, *11*, 2827−2836.
(56) Johnson, S. A.; Ollivier, P. J.; Mallouk, T. E. *Science* **1999**, *283*, 963.
(57) Marcou, J. *Plastic Optical Fibres: Practical Applications*; John Wiley & Sons: Masson, 1997.
(58) Tripathy, S.; Kim, D. Y.; Li, L.; Kumar, J. *Pure Appl. Chem.* **1998**, *70*, 1267.
(59) Kawai, H.; Suzuki, M.; Yoshida, A. *Proc. SPIE* **1997**, *3135*, 42.
(60) Fantone, S. D. *Proc, SPIE* **1983**, *406*, 82.
(61) Blough, C.; Faklis, D.; Mack, S. K.; Michaels, R. L.; Ward, S. J. *Proc. SPIE* **1995**, *2600*, 50.
(62) Brinker, C. J.; Scherer, G. W. *Sol−gel Science: The Physics and Chemistry of Sol−Gel Processing*; Academic Press: Boston, 1990.
(63) Bullock, D. L.; Shih, C.-C.; Margulies, R. S. *J. Opt. Soc. Am. B* **1993**, *10*, 399.
(64) Lei, X.; Li, H.; Ding, F.; Zhang, W.; Ming, N. *Appl. Phys. Lett.* **1997**, *71*, 2889.
(65) Dowling, J. P.; Scalora, M.; Bloemer, M. J.; Bowden, C. M. *J. Appl. Phys.* **1994**, *75*, 1896.
(66) Hirayama, K.; Hamano, T.; Aoyagi, Y. *Appl. Phys. Lett.* **1996**, *69*, 791.
(67) Jiang, P.; Bertone, J. F.; Hwang, K. S.; Colvin, V. L. *Chem. Mater.* **1999**, *11*, 2132.

ensures that the resulting polymer films meet the specifications for optical characterization. This strategy also relies on the use of silica, not latex, spheres as a template. This makes it possible to remove the template at room temperature by treatment with dilute hydrofluoric acid. Thus, macroporous films of a wide variety of polymers can be cast through either photoinitiated or thermally initiated polymerization. Visualization of the macroporous polymers using scanning electron microscopy (SEM) reveals that the samples exhibit not only an ordered void structure from the silica spheres, but also a uniform distribution of pores which form around points where the spheres once touched. The sizes of these small pores are a sensitive function of monomer viscosity. They may be of utility in other nonoptical applications, such as size selective filters or electrophoretic separations media. Optical transmission studies of the polymer/air sphere materials illustrate the existence of a optical stop band, in which strong diffraction effects limit the optical transmission of the film. These transmission spectra can be accurately modeled by calculations based on the scalar wave approximation.[68−70]

Experimental Section

Materials and Substrates. All solvents and chemicals are of reagent quality and are used without further purification except for tetraethoxysilane (Alfa, 99%) which is freshly vacuum distilled before use. Ethanol (200 proof) is obtained from Pharmaco Products. Ammonium hydroxide (29.6%) and hydrofluoric acid (49%) are obtained from Fisher. Commercially available monomers are used: methyl methacrylate (Aldrich), methyl acrylate (Aldrich), styrene (Acros), NOA 60 (polyurethane, Norland), F113 (epoxy, Tra-Con), and epoxy resin (Hardman). 2,2-Diethoxyacetophenone (Aldrich, 95%) is used as UV photoinitiator. The refractive indices of the resultant polymers are as follows: PMMA, 1.49;[71] PMA, 1.472−1.480;[71] polystyrene, 1.59−1.592;[71] polyurethane,1.5−1.6;[71] and epoxy, 1.55−1.60.[71] Twenty-milliliter scintillation vials and glass microslides (75 × 25 × 1 mm) are obtained from Fisher and cleaned in a chromic−sulfuric acid cleaning solution (Fisher) overnight, rinsed with Milli-Q water (18.2 MΩ cm^{-1}), and dried in a stream of nitrogen. Teflon spacers (0.1 mm) are obtained from Aldrich.

Instrumentation. Scanning electron microscopy and EDAX are carried out on a Philips XL30 ESEM. Transmission spectra are obtained by using an Ocean Optics ST2000 fiber optic UV−near-IR spectrometer. An Oriel model 60000 UV lamp with 68806 basic power supply is used to initiate the polymerization. A Fisher Isotemp 2150 circulator and an acrylic open bath are used to control the polymerization temperature to ±0.5 °C accuracy. A CrC-100 sputtering system has been used to sputter a thin layer (3−4 nm) of gold on the samples before SEM analysis.

Colloid Synthesis and Colloidal Crystal Growth. Monodisperse SiO_2 nanospheres are synthesized following the Stober−Fink−Bohn[72] method. Nanospheres with diameters ranging from 200 to 400 nm and relative standard deviation smaller than 5% are obtained through strict control of the reaction conditions.[73] The methods described in our previous paper[67] are used to fabricate three-dimensionally ordered planar colloidal crystals with thickness ranging from one monolayer to 50 μm. In short, a microslide is dipped into a purified silica/ethanol dispersion. Through convective self-assembly,[74−76] an iridescent colloidal single-crystal grows on the surface within 3−4 days while ethanol evaporates. By adjusting particle size and volume fraction, the thickness of the resulting film can be precisely controlled. Typically films of 10−50 layers can be prepared in a single coating, while successive coats can make films up to 200 layers (about 50 μm depending on sphere size) (see Figure 1). These materials were used as templates for preparing macroporous polymers.

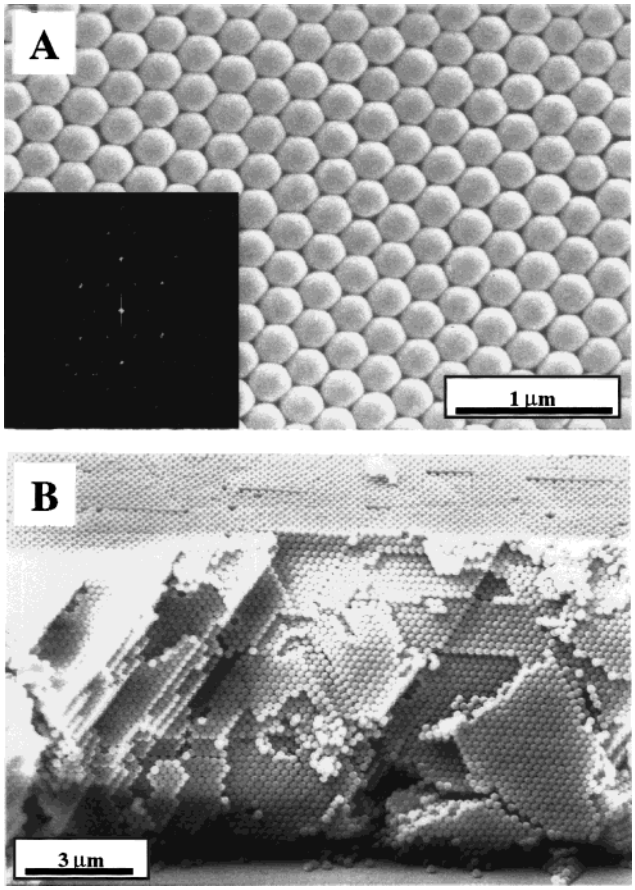

Figure 1. Typical scanning electron micrograph (SEM) images of a SiO_2 colloidal single-crystal template (298.6 nm) for fabricating macroporous polymers: (a) top view (×30 000) with inset showing the FFT of a low magnification image of a 40 × 40 μm^2 region and (b) side view (×6000) of the same sample, from which the film thickness can be determined.

Fabrication of Three-Dimensionally Ordered Macroporous Polymers. A schematic outline of the procedure for producing three-dimensionally ordered macroporous polymers is shown in Figure 2. The microslide with SiO_2 colloidal crystal on its surface is covered by another microslide and dipped in 1−2 mL of a monomer. Capillary forces draw the liquid monomer into the void spaces between the silica particles. Filling times range from several seconds for a low viscosity precursor such as styrene to 5−10 min for a high viscosity monomer such as NOA 60. Because of refractive index matching between silica and monomer, the cell becomes transparent. The prepolymers are then cross-linked thermally at 60 °C or by exposure to UV light (320 W) for several hours. Afterward one or both microslides are carefully removed and the free-standing polymer film is soaked in 4% hydrofluoric acid solution (about 15 mL) overnight to remove the SiO_2. The resulting macroporous polymer is air-dried. Depending on the properties of different polymers, the products can be rigid (poly(methyl methacrylate) and poly(styrene)) or flexible (poly(urethane)). To form a stronger self-standing macroporous polymer, a 0.1-mm Teflon spacer

(68) Satpathy, S.; Zhang, Z.; Salehpour, M. R. *Phys. Rev. Lett.* **1990**, *64*, 1239.
(69) Mittleman, D.; Bertone, J.; Jiang, P.; Hwang, K.; Colvin, V. *J. Chem. Phys.* **1999**, *111*, 345.
(70) Bertone, J. F.; Jiang, P.; Hwang, K. S.; Mittleman, D. L.; Colvin, V. L. *Phys. Rev. Lett.* **1999**, *83*, 300.
(71) Brandrup, J.; Immergut, E. H. *Polymer Handbook*; John Wiley & Sons: New York, 1975.
(72) Stober, W.; Fink, A.; Bohn, E. *J. Colloid Interface Sci.* **1968**, *26*, 62.
(73) Bogush, G. H.; Tracy, M. A.; Zukoski IV, C. F. *J. Non-Cryst. Solids* **1988**, *104*, 95.
(74) Denkov, N. D.; Velev, O. D.; Kratchevsky, P. A.; Ivanov, I. B.; Yoshimura, H.; Nagayama, K. *Nature* **1993**, *361*, 26.
(75) Denkov, N. D.; Yoshimura, H.; Nagayama, K. *Ultramicroscopy* **1996**, 147.
(76) Dimitrov, A.; Nagayama, K. *Chem. Phys. Lett.* **1995**, *243*, 462.

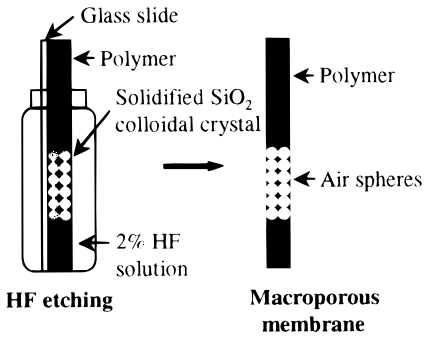

Figure 2. A schematic outline of the procedure for making macroporous polymers.

can be used to separate the two microslides. The films exhibit striking iridescence due to Bragg diffraction of visible light by the ordered air spheres in the polymer. The sizes of the spherical pores and the thickness of the macroporous polymer can be controlled by changing the thickness and sphere size of the template silica film.

Controlling the Size of Smaller Interconnecting Pores. By adjusting polymerization temperature, the size of smaller interconnecting pores can be controlled. A Fisher Isotemp 2150 circulator and an acrylic open bath are used to control the polymerization temperature of NOA 60. At low temperatures the prepolymers are very viscous and take ~5 min to fill the template while at high temperatures they are less viscous, and fill the cell in several seconds. After the monomer equilibrates for 30 min in the isotemp bath, the monomer is polymerized by exposure to UV light as described above.

Characterization of the Macroporous Polymers. The macroporous polymers can be affixed to conductive carbon tape and prepared for scanning electron microscopy by sputtering a thin layer (3−4 nm) of gold onto the surface. A Philips XL30 ESEM has been used to evaluate the resulting macroporous polymers. The samples are tilted 30−40° to obtain the cross-sectional images. In situ EDAX is used to evaluate the amount of residual silica. To determine the diameter and standard deviation of smaller inner pores, over 200 pores are sized using SEM.

The optical properties of the macroporous poly(methyl methacrylate) films are evaluated by transmission spectroscopy using an Ocean Optics ST2000 fiber optic UV−near-IR spectrometer. Free-standing macroporous PMMA films are sandwiched by two microslides to ensure flatness. Pure PMMA films with the same thickness are used as references.

Results

The quality of any material formed via template-directed synthesis depends sensitively on the order and properties of the starting template. Figure 1 shows a typical scanning electron micrograph (SEM) of the top and side views of one of our templates, a colloidal silica single crystal. In this instance, 298-nm silica spheres are organized into a close-packed arrangement with long-range order both parallel and perpendicular to the glass substrate. While SEM provides a good picture of the sample quality over 10 μm, the assessment of order over a larger range is best found in Fourier transform analysis of low magnification SEM (40 × 40 μm^2). Such data is shown in the inset of Figure 1a; sharp peaks in the Fourier transform confirm long-range crystalline order. SEM studies over adjoining regions spanning more than 5 mm reveal no detectable grain boundaries.[67] While it is clear that the samples are also crystalline in the cross-sectional view (Figure 1b), it should noted that perspective views such as these cannot distinguish between the hexagonal close-packed structure (ABABAB) and the face-centered cubic structure (ABCABCABC).

These silica−air crystals can serve as templates for the formation of macroporous polymers as illustrated in Figure 2. Figure 3 shows a typical SEM top and side view of a macroporous poly(styrene) film made by using a 330-nm silica

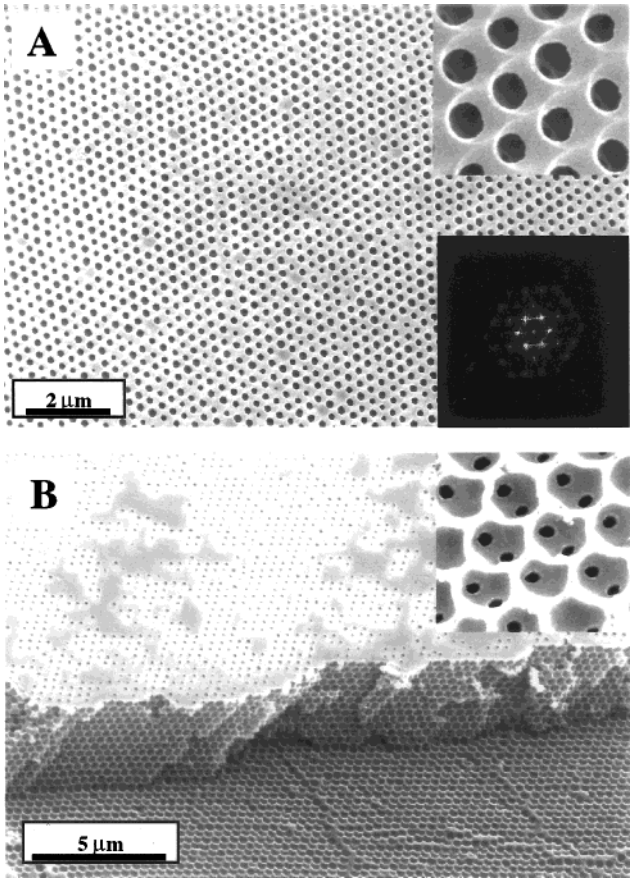

Figure 3. Scanning electron micrograph (SEM) images of a typical macroporous poly(styrene) membrane, formed using a 330.2 nm SiO_2 colloidal crystal as a template: (a) top view (×8000), with upper inset showing higher magnification (×100 000) and lower inset showing the FFT of a low magnification image of a 40 × 40 μm^2 region, and (b) side view (×6000), with inset showing the interconnecting inner pores at higher magnification (×100 000).

colloidal crystal as a template. The material clearly has retained the three-dimensional crystalline order of the template and exhibits ordered close packing of air spheres in the polymer. Sharp peaks in the FFT of even larger length scale (40 × 40 μm^2, see the bottom inset in Figure 3a) demonstrate the long-range crystalline order. The marks left by template silica balls shown in the upper inset of Figure 3a are clearly visible.

Membranes up to several square centimeters in area are easily prepared using larger template crystals. Figure 5 shows a photograph of a macroporous poly(methyl methacrylate) film grown using a 330 nm silica colloidal crystal as a template. The reflected colors are caused by Bragg diffraction of visible light by the array of air spheres. Several colors are apparent in the image. This is because the film is flexible and slightly curved in this example, so the angle of incidence of the illuminating white light varies with respect to the crystal planes.

Since the starting template can be made from spheres of variable size, the resulting macroporous polymers have tunable void volume. Figure 4 shows the SEM cross-sectional images of macroporous poly(methyl acrylate) films made by using 324 nm silica colloidal crystals of different thickness (10 layers for Figure 4a and 24 layers for Figure 4b) as templates. Films up to 50 μm can be made using these templates. An advantage of the thicker films is that they are sturdier and can be more readily handled as free-standing films. Figure 6 illustrates that these macroporous polymers can be made with different void sizes.

An interesting feature of these samples is the smaller uniform

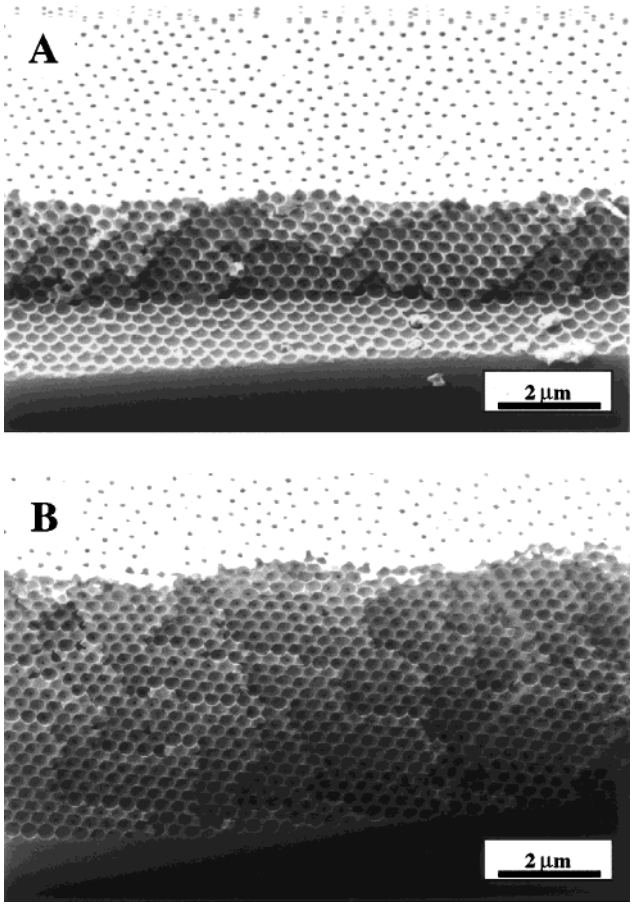

Figure 4. Typical scanning electron micrograph (SEM) cross-sectional images of two macroporous poly(methyl acrylate) membranes made using the same size (324.8 nm) silica templates with different thickness: (a) 10 layers and (b) 24 layers.

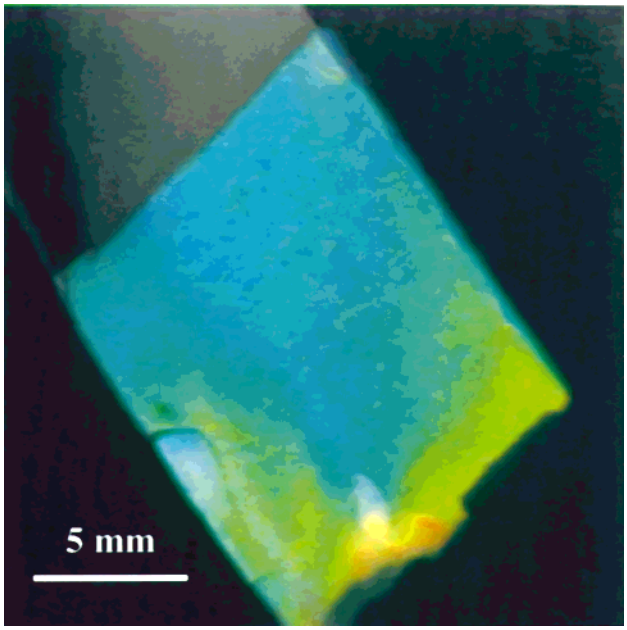

Figure 5. A photograph showing the colors reflected from a macroporous poly(methyl methacrylate) (PMMA) film made by 330.2 nm silica template. The variation in color arises from the fact that the film is curved.

inner pores, which interconnect the larger air spheres. Figure 6 shows SEM top views of macroporous poly(styrene) films made by using 260 and 330 nm silica single crystal as templates.

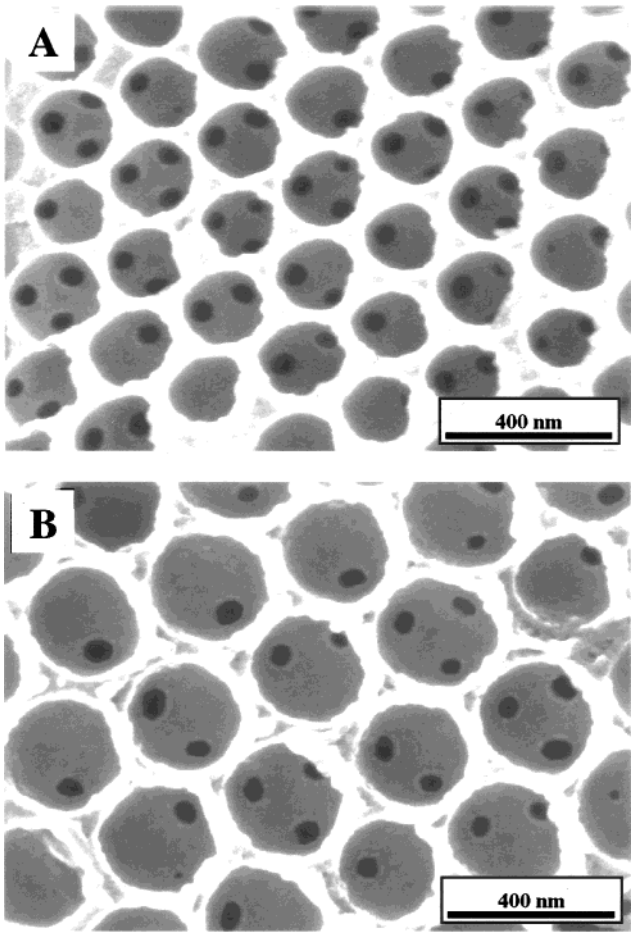

Figure 6. Scanning electron micrograph (SEM) top view images of the inner layers of two macroporous poly(styrene) membranes made using silica templates with different sphere diameters. This shows the insensitivity of the size of the interconnecting inner pores to the size of the template silica spheres: (a) 260.4 nm silica template produced 55.8 nm (±6.8%) inner pores and (b) 330.2 nm silica template produced 57.9 nm (±7.4%) inner pores.

These images are different from Figure 3a because the samples were prepared so that the interior layers of the polymer rather than the surface layers are visible. The smaller inner pores appear at nearly regular spacing in the polymer, wherever silica spheres were in closest proximity to one another. Over 200 inner pores were counted and sized in the SEM, providing average sizes and distributions. Figure 6a shows a sample with 55.8 ± 3.8 nm inner pores made by 260 nm template silica and Figure 6b shows a sample with 57.9 ± 4.3 nm inner pores made by 330 nm template silica. Some of these pores are missing or very small, likely the result of defects or silica spheres that were not in perfect contact. These defects, which are present at ∼20% of the total sites, are not so prevalent as to disrupt the interconnected pore network.

The temperature of the initial monomer solution has a significant effect on the size of the internal pores. Figure 7 shows that the size of the smaller pores in macroporous NOA 60, a commercial polyurethane, could be varied through control of monomer temperature. For a given sample of silica colloidal crystals (353-nm diameter), very viscous NOA 60 at 22.5 °C produced 117.6 ± 8.3 nm inner pores. Less viscous monomer at 40.0 °C made 90.6 ± 6.5 nm pores and at 70 °C, where the monomer was very fluid, inner pores of 60.7 ± 4.9 nm were produced. Other parameters, such as the shrinkage of the monomer upon polymerization, as well as its ability to wet the silica surface, had much less effect on the observed morphology.

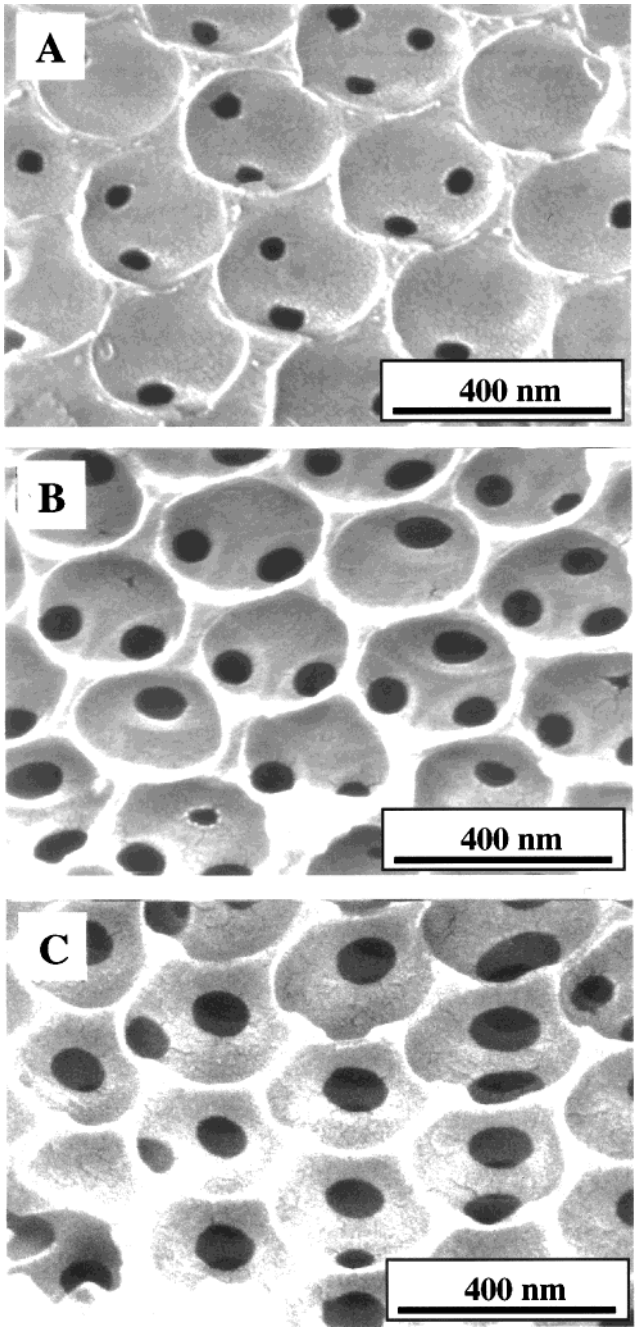

Figure 7. Scanning electron micrograph (SEM) top view images of the inner layers of three macroporous poly(urethane) membranes made using identical silica templates (353.0-nm sphere diameter) at different polymerization temperatures. This illustrates the systematic change in the sizes of the inner pores with polymerization temperature. This is attributed to changes in the viscosity of the prepolymer: (a) $T = 70.0$ °C, pore diameter = 60.7 nm (±8.1%); (b) $T = 40.0$ °C, pore diameter = 90.6 nm (±7.2%); and (c) $T = 22.5$ °C, pore diameter = 117.6 nm (±7.1%).

Optical studies of these samples illustrate the diffractive properties of the matrix and provide additional evidence of the high crystalline quality of these samples. Figure 8 shows the optical transmission spectra for three macroporous polymer samples made from silica spheres ranging from 311 to 360 nm in diameter. A small incoherent scattering background was subtracted from these data to facilitate comparison with a theoretical model of photonic band gap behavior (dashed lines), described further below. Figure 9 shows the predicted peak position, λ_{peak}, versus sphere diameter; again the data is in agreement with a model which assumes a perfect three-dimensional lattice of ordered air spheres in a polymer matrix.

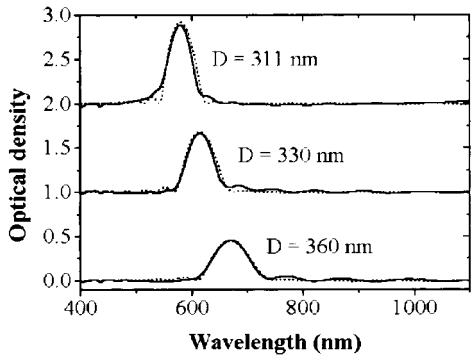

Figure 8. Experimental (solid lines) and calculated (dotted) optical transmission spectra at normal incidence of macroporous poly(methyl methacrylate) membranes. The diameters of the air spheres in the three samples are shown. All three calculated curves have been scaled by an overall multiplicative factor of 0.75, as described in the text. Otherwise, these calculations contain no adjustable parameters. The excellent agreement between the observed and calculated bandwidths is further evidence for the high quality of the samples.

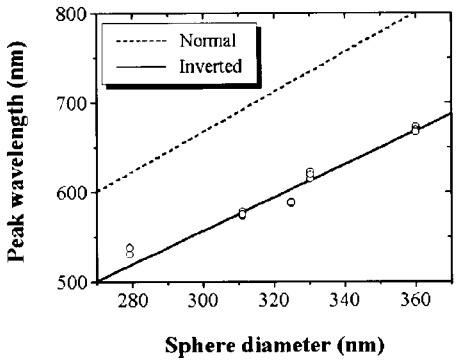

Figure 9. Wavelength at which the optical transmission spectrum peaks, λ_{peak}, as a function of sphere diameter. The open circles are experimental points measured at normal incidence. The solid curve shows the calculated value of λ_{peak} for the inverted macroporous structures, while the dashed curve shows the value for the silica sphere templates.

One important issue for many applications is the net void volume, or surface area, in these systems; energy-dispersive X-ray analysis (EDAX) of the macroporous films show only trace amounts of silica (less than 0.7%), indicating that the treatment does remove almost all of the silica. This is not surprising due to high dissolution rate of silica in aqueous HF ($k_1 = 5 \times 10^{-8}$ g SiO_2 s^{-1} cm^{-2} M_{HF}^{-1})[77] and the internal connection between silica spheres. Additionally, the predicted optical spectra are highly sensitive to the volume fraction occupied by the polymer. The predictions shown in Figures 8 and 9 assume that the air spheres are close-packed, and that the polymer fills the remaining ~26% of the total volume. The good agreement with experimental results provides further evidence that the polymer effectively templates against the colloidal crystal.

Discussion

Macroporous Polymers with Uniform Thickness and Pore Size. A template method such as this one provides a simple

(77) Iler, R. K. *The Chemistry of Silica: Solubility, Polymerization, Colloid and Surface Properties, and Biochemistry*; John Wiley & Sons: New York, 1979.

and versatile route for the production of macroporous polymers. A comparison of Figures 1 and 3 clearly shows that the high quality of the initial silica colloidal crystals leads to high-quality porous polymers. Moreover, since the template thickness and sphere size can be controlled, so can the macroporous structure. Void sizes ranging from 200 to 400 nm in diameter have been achieved, with good thickness uniformity across 1 cm in all cases (Figure 5). Monodisperse silica spheres can be made ranging from 20 nm[78] up to several micrometers in diameter.[73] If high-quality templates of the larger and smaller silica can be prepared, then void sizes over the entire nanometer size range should be feasible.

An important issue for many applications of macroporous polymers, especially those prepared in a thin-film format, is that the resulting films must be strong and resistant to cracking. While the mechanical properties have not been quantified here, this method allows for the use of any monomer whose resulting polymer is not soluble in hydrofluoric acid. Thus, glassy polymers (polystyrene, $T_g \approx 94.8$ °C)[71] as well as rubbery polymers (poly(urethane), $T_g \approx 24.5-25.0$ °C)[79] work equally well in templating against the colloidal crystal. In addition, the initial template can be prepared in thickness up to 50 μm. Macroporous methacrylate polymers made with these thickness are free-standing and flexible. Template crystals can be prepared with even greater thickness (up to 1 mm); however their long-range crystalline order begins to degrade above 50 μm. In addition, polycrystalline colloidal crystals of silica are routinely prepared in millimeter capillary tubes as opposed to our planar thin film geometry.[80] While such samples would not be ideal for optical studies, they may be more suitable for other applications requiring macroporous media.

Small Interconnected Pore Structure Arises from Monomer Wetting. Given the potential importance of the interconnection pores in nonoptical applications, primarily separation technologies, we investigated whether and over what range their size could be controlled. From their placement in the larger voids it is apparent that these small pores are located where the template silica spheres were in closest proximity. One possible explanation for their origin is that the initial monomer solution could not wet the silica sphere surfaces completely, leading to gaps in its filling of the template. Fluid viscosity is known to be an important factor governing the effective filling of porous materials; more viscous liquids are less able to completely absorb into the available free space due to both wetting and capillary phenomena.[81−84] Alternatively, polymerization shrinkage could result in the formation of the pores. The three monomers employed in this work undergo 20−30% volume shrinkage upon polymerization;[85] as the silica template is effectively incompressible, thin areas of polymer such as those located between spheres could yield, due to shrinkage, the pore structure observed.

To evaluate these issues, NOA 60, a particularly viscous monomer, was polymerized at different temperatures. Temperature has a large effect on monomer viscosity,[71,86] and thus the monomer fills the porous template faster at higher temperatures. Figure 7 shows the systematic decrease in pore size as the temperature is increased. This observation illustrates that monomer viscosity is an important consideration in the formation of the smaller pores, and by manipulating this parameter inner pore sizes can be controlled. Efforts to create smaller pores using very low viscosity monomers, however, were not successful and average pore diameters of 50 nm were typical. It may be that this lower limit is indeed the result of polymerization shrinkage. If so, the creation of inner pores whose diameters are smaller than 50 nm will require low shrinkage monomers.

Optical Properties of Macroporous Polymers. Because of the ordering of the air spheres within the polymer, these samples exhibit diffraction phenomena that lead to striking optical properties. The most prominent is the presence of a strong diffraction peak in the optical spectrum. Certain basic properties of these systems can be well described by Bragg's law. At normal incidence (where $\sin \theta_{inc} = 1$), the spectral position of the peak in the optical density, λ_{peak}, can be found from

$$\lambda_{peak} = 2n_{eff}d_{111} \quad (1)$$

where n_{eff} is the average refractive index of the entire medium (air and polymer) at optical frequencies and d_{111} is the interlayer spacing of the air spheres along the (111) direction. This spacing is related to the sphere diameter D by $d_{111} = \sqrt{2/3}D$ for any close-packed structure.

While Bragg's law explains the spectral position of the peak, a theoretical treatment appropriate to strongly diffracting layers is necessary to provide a quantitative model of the optical spectra. The scalar wave theory developed for periodic dielectric structures[68,87] can be easily applied to these materials. In short, Maxwell's equations are solved for a periodic dielectric assuming that one may neglect diffraction from all but one set of crystalline planes (in this case, the (111) planes). While this approximation is not entirely correct, the model is tractable and is appropriate for comparison with normal-incidence transmission spectra. In particular, although this theory always predicts a larger optical density than observed, the predicted spectral bandwidths are in good agreement with observations.[69] Thus, this formalism can be used to evaluate whether the observed bandwidths are controlled by defects in the sample or are intrinsic to the film. In principle, the calculation contains no adjustable parameters, since the size of the spheres and the sample thickness are independently determined from SEM measurements, and the refractive index of the polymer is known. However, because of the known difficulties in predicting the magnitude of the peak optical density, an overall multiplicative scaling factor is used. This facilitates comparisons of the measured and calculated bandwidths.

The predictions of the scalar wave approximation are compared to experimental data in Figure 8. The samples used to obtain these data (solid lines) were all thin, on the order of 9−12 layers. All three theoretical curves (dotted lines) have been scaled by a multiplicative factor of 0.75, but otherwise there are no adjustable parameters. Remarkable agreement between theory and experiment provides evidence that these

(78) Arriagada, F. J.; Osseo-Asare, K. *J. Dispersion Sci. Technol.* **1994**, *15*, 59.
(79) Wirpsza, Z. *Polyurethanes: Chemistry, Technology and Applications*; Ellis Horwood: New York, 1993.
(80) Mayoral, R.; Requena, J.; Moya, o. S.; Lopez, C.; Cintas, A.; Miguez, H.; Meseguer, F.; Vazquez, L.; Holgado, M.; Blanco, A. *Adv. Mater.* **1997**, *9*, 257.
(81) Tzimas, G. C.; Matsuura, T.; Avraam, D. G.; Van Der Brugghen, W.; Constantinides, G. N.; Payatakes, A. C. *J. Colloid Interface Sci.* **1997**, *189*, 27.
(82) Nieh, S. Y.; Ybarra, R. M.; Neog, P. *Macromolecules* **1996**, *29*, 320.
(83) Samsonov, V. M. *Colloid J.* **1997**, *59*, 520.
(84) Massimo, S. *Mater. Struct.* **1998**, *32*, 162.
(85) Mark, J. E. *Physical Properties of Polymers Handbook*; Woodbury: New York, 1996.
(86) Barrow, G. M. *Physical Chemistry*, 6th ed.; McGraw-Hill: New York, 1996.
(87) Shung, K. W. K.; Tsai, Y. C. *Phys. Rev. B* **1993**, *48*, 11265.

samples are not highly defective; in addition, it rules out the possibility that residual silica was left behind. Finally, optical characterization of this type illustrates that the film did not undergo significant dimensional changes during the HF treatment and thus faithfully reproduced the starting template. Figure 9 shows the predicted and measured spectral positions of the optical stop bands, as a function of sphere diameter, obtained from data such as that shown in Figure 8. The solid line is the prediction from the scalar wave theory, which is nearly identical to that obtained from Bragg's law, eq 1 above, for films thicker than ~20 layers.[69] For reference, the dashed line shows the predicted spectral positions for the templates ("normal" samples, with silica spheres surrounded by air, as opposed to "inverted" or macroporous samples). The ~100 nm shift between the two is a result of the substantial decrease in n_{eff}, resulting from the lower volume fraction occupied by the polymer in the "inverted" samples.

Conclusion

Macroporous polymer films suitable for optical applications can be made using silica colloidal crystals as templates. SEM micrographs show the presence of ordered voids whose diameter matches the diameter of the starting silica spheres. Optical characterization provides verification of the uniform nature of the sample and confirms that the initial template geometry is retained after templating. One feature of these samples is that the air spheres are interconnected through small windows whose diameters range from 50 to 120 nm, depending on polymerization conditions. These films, larger 100 nm voids connected by smaller pores, are reminiscent of many inorganic zeolites though with a much larger length scale. This suggests that these films may be valuable for large-molecule separation processes, where the interconnecting pores provide optimal flow and improved efficiencies.

JA9903476